Inorganica Chimica Acta, 204 (1993) 175–179

The synthesis and characterization of an $\mathrm{Mo\overset{4}{-}MoCl_4(L\text{-}L)_2}$ compound with $\mathrm{L\text{-}L = Ph_2PCH_2PMe_2}$

F. A. Cotton*, Judith L. Eglin** and Chris A. James†

Department of Chemistry and The Laboratory for Molecular Structure and Bonding, Texas A&M University, College Station, TX 77843 (USA)

(Received July 13, 1992)

Abstract

The preparation and structural characterization of a new $\mathrm{Mo\overset{4}{-}Mo}$ complex with an interesting asymmetric bidentate phosphine $\mathrm{Mo\overset{4}{-}MoCl_4(\mu\text{-dmdppm})_2}$ (dmdppm = $\mathrm{Ph_2PCH_2PMe_2}$) is reported. The $\mathrm{Mo\overset{4}{-}Mo}$ bond distance in $\mathrm{Mo\overset{4}{-}MoCl_4(\mu\text{-dmdppm})_2}$ (2.1523(9) Å) is longer than those in either $\mathrm{Mo\overset{4}{-}MoCl_4(\mu\text{-dppm})_2}$ (2.138(1) Å) or $\mathrm{Mo\overset{4}{-}MoCl_4(\mu\text{-dmpm})_2}$ (2.125(4) Å) due to the presence of a twist about the $\mathrm{Mo\overset{4}{-}Mo}$ axis of 17.56°. The crystal structure of $\mathrm{Mo\overset{4}{-}MoCl_4(\mu\text{-dmdppm})_2}$ is fully described. Crystallographic data for this compound are as follows: (1) $P2_1/c$ with $a = 12.552(6)$, $b = 17.223(3)$, $c = 18.582(9)$ Å, $V = 3989(3)$ Å^3 and $Z = 4$.

Introduction

An interesting structural aspect of $\mathrm{Mo\overset{4}{-}MoX_4(\mu\text{-L-L})_2}$ molecules is the staggered or partially staggered geometry that can be adopted about the metal–metal axis [1, 2]. The presence of a twist about the $\mathrm{Mo\overset{4}{-}Mo}$ axis is difficult to predict before a complex has been characterized, but in general compounds where L-L forms a three atom bridge have either a small torsional angle or none at all. Complexes with L-L bridges of more than three atoms tend to have larger torsional angles [1–3]. For the quadruple bond ($\sigma^2\pi^2\delta^2$), the δ^2 contribution to the bond strength is sensitive to the degree that the molecule is rotated from the eclipsed conformation. In fact, there is a direct correlation between the $\mathrm{Mo\overset{4}{-}Mo}$ bond length and the cosine of twice the torsional angle [1].

$\mathrm{Mo\overset{4}{-}MoCl_4(\mu\text{-dppm})_2}$ and $\mathrm{Mo\overset{4}{-}MoCl_4(\mu\text{-dmpm})_2}$ with the ligands $\mathrm{Ph_2PCH_2PPh_2}$ (dppm) and $\mathrm{Me_2PCH_2PMe_2}$ (dmpm) have both been structurally characterized and both have an eclipsed geometry [4, 5]. A new complex $\mathrm{Mo\overset{4}{-}MoCl_4(\mu\text{-dmdppm})_2}$ has been made with the asymmetric bidentate phosphine ligand $\mathrm{Ph_2PCH_2PMe_2}$ (dmdppm), which can be considered as a hybrid between the ligands dppm and dmpm. While one might have predicted that many of the structural characteristics of the complex would fall halfway between those of $\mathrm{Mo\overset{4}{-}MoCl_4(\mu\text{-dmpm})_2}$ and $\mathrm{Mo\overset{4}{-}MoCl_4(\mu\text{-dppm})_2}$, this is not the case due to the presence of a torsional angle in $\mathrm{Mo\overset{4}{-}MoCl_4(\mu\text{-dmdppm})_2}$. The synthesis, characterization and crystal structure of this new quadruply bonded dimolybdenum(II) compound are reported and comparisons are made with $\mathrm{Mo\overset{4}{-}MoCl_4(\mu\text{-dppm})_2}$ and $\mathrm{Mo\overset{4}{-}MoCl_4(\mu\text{-dmpm})_2}$.

Experimental

Preparation of compounds

All manipulations were carried out under an atmosphere of argon unless otherwise specified. Standard Schlenk and vacuum line techniques were used. Commercial grade solvents, except alcohols and dichloromethane, were dried over and freshly distilled from potassium/sodium benzophenone ketyl prior to use. Alcohols and dichloromethane were dried over magnesium turnings and phosphorus pentoxide, respectively, and freshly distilled prior to use. $\mathrm{Mo_2Cl_4(PPh_2Me)_4}$ [6] and dmdppm [7] were prepared by published procedures. Diphenylmethylphosphine was purchased from Strem Chemicals and used without any further purification.

The ^{31}P{^{1}H} NMR (81 MHz) spectra were recorded on both a Varian XL-200 and 400 spectrometer. The ^{31}P{^{1}H} NMR chemical shift values were referenced

---

*Author to whom correspondence should be addressed.

**Mississippi State University, Mississippi State, MS 39762, USA.

†Los Alamos National Laboratory, INC-4 Los Alamos, NM 87545, USA.

0020-1693/93/$6.00

externally and are reported relative to 85% H_3PO_4. UV–Vis spectra were recorded on a Cary 17D spectrophotometer.

$\text{Mo}\overset{4}{-}\text{MoCl}_4(\mu\text{-dmdppm})_2$

A 0.070 g (0.062 mmol) sample of $\text{Mo}_2\text{Cl}_4(\text{PPh}_2\text{Me})_4$ was dissolved in 20 ml of THF. To the blue solution, 0.124 mmol of dmdppm in 1 ml of THF was added. An aliquot of the solution was placed in a 10 mm NMR tube and the reaction monitored by $^{31}\text{P}\{^1\text{H}\}$ NMR spectroscopy. At room temperature, the reaction reached completion after 5 h. The green–blue reaction mixture was filtered and then placed in long glass tubes and layered with a benzene/methanol mixture (1:8). After several weeks at 0 °C, long, thin, blue–green needles of $\text{Mo}\overset{4}{-}\text{MoCl}_4(\mu\text{-dmdppm})_2$ were obtained. These crystals were used to characterize the compound by X-ray diffraction, UV–Vis and $^{31}\text{P}\{^1\text{H}\}$ NMR spectroscopy. No attempts were made to optimize the yield in this reaction.

Crystallographic studies

A blue–green needle shaped crystal was selected, coated with epoxy cement and mounted on the end of a glass fiber. Single-crystal diffraction experiments were conducted using an Enraf-Nonius CAD-4S automated diffractometer with Mo Kα radiation. Routine unit cell identification and intensity data collection procedures were followed utilizing the options specified in Table 1 and the general procedures previously described [8]. Lattice dimensions and Laue symmetry were verified using axial photographs. Three standard reflections were measured every hour during data collection to monitor any gain or loss in intensity but no correction was applied since the loss in intensity was 0.9%. Corrections for Lorentz, polarization and absorption effects were applied. The latter correction was based on azimuthal scans of several reflections with diffractometer angle χ near 90° [9]. The final refinement factors after convergence are listed in Table 1. Table 2 contains positional and thermal parameters for non-hydrogen atoms and their e.s.d.s for $\text{Mo}\overset{4}{-}\text{MoCl}_4(\mu\text{-dmdppm})_2$.

TABLE 1. Crystal data for $\text{Mo}\overset{4}{-}\text{MoCl}_4(\mu\text{-dmdppm})_2$

Chemical formula	$\text{Mo}_2\text{Cl}_4\text{P}_4\text{C}_{32}\text{H}_{46}$
Formula weight	888.34
Space group (No.)	$P2_1/c$(14)
a (Å)	12.55(8)
b (Å)	17.22(6)
c (Å)	18.58(5)
β (°)	96.07(1)
V (Å^3)	3989(4)
Z	4
ρ_{calc} (g cm^{-3})	1.479
μ(Mo Kα) or (Cu Kα) (cm^{-1})	10.631
T (°C)	23 ± 2
λ (Å)	0.71073
$R(F_o)$[a]	0.0389
$R_w(F_o)$[b]	0.0412

[a] $R = \Sigma\,||F_o| - |F_c||/\Sigma|F_o|$. [b] $R_w = [\Sigma w(|F_o| - F_c|)^2/\Sigma w|F_o|^2]^{1/2}$; $w = 1/\sigma^2(|F_o|)$.

TABLE 2. Positional and thermal parameters for non-hydrogen atoms of $\text{Mo}\overset{4}{-}\text{MoCl}_4(\mu\text{-dmdppm})_2$

Atom	x	y	z	B (Å^2)[a]
Mo(1)	0.23914(5)	0.08629(4)	0.33003(3)	2.85(2)
Mo(2)	0.32326(5)	0.18167(4)	0.38579(4)	2.99(2)
Cl(1)	0.2004(2)	−0.0035(1)	0.4223(1)	3.92(5)
Cl(2)	0.2128(2)	0.1055(2)	0.2018(1)	5.00(6)
Cl(3)	0.3897(2)	0.1310(1)	0.5028(1)	4.27(5)
Cl(4)	0.3204(2)	0.2962(1)	0.3126(1)	5.36(6)
P(1)	0.0499(2)	0.1339(1)	0.3450(1)	3.21(5)
P(2)	0.4021(2)	−0.0012(1)	0.3148(1)	3.47(5)
P(3)	0.5079(2)	0.1469(1)	0.3517(1)	3.26(5)
P(4)	0.1695(2)	0.2385(1)	0.4493(1)	3.75(5)
C(1)	0.000(3)	0.462(2)	0.566(1)	18.8(3)*
C(2)	0.093(2)	0.506(2)	0.545(2)	18.8(3)*
C(3)	0.081(2)	0.539(2)	0.477(2)	18.8(3)*
C(4)	0.571(2)	0.467(2)	0.457(1)	18.8(3)*
C(5)	0.464(3)	0.442(1)	0.451(1)	18.8(3)*
C(6)	0.6044(9)	0.529(2)	0.502(2)	18.8(3)*
C(21)	0.4350(7)	−0.0189(6)	0.2235(5)	5.1(2)
C(22)	0.4039(7)	−0.0992(4)	0.3515(5)	4.4(2)
C(41)	0.1919(8)	0.2517(6)	0.5472(5)	5.8(3)
C(42)	0.1143(7)	0.3309(5)	0.4188(5)	5.1(2)
C(104)	0.0573(6)	0.1707(5)	0.4372(4)	3.9(2)
C(111)	−0.0137(4)	0.2128(4)	0.2913(3)	3.7(2)
C(112)	−0.1120(4)	0.2410(4)	0.3083(3)	5.1(2)
C(113)	−0.1598(4)	0.3045(4)	0.2708(3)	6.3(3)
C(114)	−0.1095(4)	0.3398(4)	0.2163(3)	6.2(3)
C(115)	−0.0112(4)	0.3117(4)	0.1993(3)	6.1(3)
C(116)	0.0367(4)	0.2482(4)	0.2368(3)	4.6(2)
C(121)	−0.0534(4)	0.0589(3)	0.3363(2)	3.4(2)
C(122)	−0.0843(4)	0.0302(3)	0.2668(2)	4.7(2)
C(123)	−0.1635(4)	−0.0268(3)	0.2559(2)	5.6(3)
C(124)	−0.2119(4)	−0.0551(3)	0.3146(2)	4.7(2)
C(125)	−0.1809(4)	−0.0264(3)	0.3841(2)	4.4(2)
C(126)	−0.1017(4)	0.0306(3)	0.3949(2)	4.1(2)
C(203)	0.5220(6)	0.0421(4)	0.3646(4)	3.5(2)
C(311)	0.5451(4)	0.1631(3)	0.2615(3)	3.7(2)
C(312)	0.4716(4)	0.1946(3)	0.2073(3)	4.4(2)
C(313)	0.5007(4)	0.2057(3)	0.1378(3)	5.6(3)
C(314)	0.6034(4)	0.1853(3)	0.1226(3)	6.7(3)
C(315)	0.6769(4)	0.1539(3)	0.1769(3)	7.4(3)
C(316)	0.6477(4)	0.1427(3)	0.2464(3)	5.7(3)
C(321)	0.6188(4)	0.1923(2)	0.4083(3)	3.4(2)
C(322)	0.6880(4)	0.1522(2)	0.4595(3)	3.9(2)
C(323)	0.7713(4)	0.1914(2)	0.5005(3)	4.3(2)
C(324)	0.7855(4)	0.2708(2)	0.4903(3)	4.5(2)
C(325)	0.7163(4)	0.3110(2)	0.4391(3)	5.1(3)
C(326)	0.6330(4)	0.2718(2)	0.3981(3)	4.4(2)

[a] Anisotropically refined atoms are given in the form of the equivalent isotropic displacement parameter defined as: $\frac{4}{3}[a^2a^{*2}B_{11} + b^2b^*B_{22} + c^2c^{*2}B_{33} + 2ab(\cos\ \gamma)a^*b^*B_{12} + 2ac(\cos\ \beta)a^*c^*B_{13} + 2bc(\cos\ \alpha)b^*c^*B_{23}]$. Starred atoms were refined isotropically.

Results and discussion

Synthesis and structure

The preparation of $Mo\overset{4}{-}MoCl_4(\mu\text{-dmdppm})_2$ is straightforward and proceeds via phosphine substitution of $Mo\overset{4}{-}MoCl_4(PPh_2Me)_4$. Of note is the head to tail arrangement of the asymmetric bridging ligand in the structure of $Mo\overset{4}{-}MoCl_4(\mu\text{-dmdppm})_2$ shown in Fig. 1. No evidence for the other possible ligand arrangement (head to head, tail to tail) was observed. The phosphine ligand, dmdppm, may be considered intermediate to dppm and dmpm. One might predict many of the structural properties of the dimolybdenum complex of dmdppm to be intermediate to those with dppm and dmpm, yet the crystal structure of $Mo\overset{4}{-}MoCl_4(\mu\text{-dmdppm})_2$ has some interesting characteristics. The most striking feature of the structure of $Mo\overset{4}{-}MoCl_4(\mu\text{-dmdppm})_2$ is the presence of the 17.56° torsional angle shown in Fig. 2 with a summary of the individual torsional angles given in Table 3.

While torsional angles are not unusual in complexes of the general type $Mo\overset{4}{-}MoX_4(\mu\text{-L-L})_2$ [1, 2, 10–12], they occur in only a few examples where only a single –CHR– group bridges the two phosphine atoms of the ligand [3, 4]. One example is the complex $Mo\overset{4}{-}Mo(NCS)_4(dppm)_2$ containing an X group composed of three atoms in a chain containing a 13° twist along the $Mo\overset{4}{-}Mo$ axis from the eclipsed configuration. $Mo\overset{4}{-}MoCl_4(tdpm)_2$ where $tdpm = Ph_2PCH(PPh_2)PPh_2$ has a torsional angle of 20°, presumably due to the bulkiness introduced by the $-PPh_2$ group in tdpm as compared to the simple $-CH_2-$ bridge in dppm [3]. In the related ditungsten chemistry, $W\overset{4}{-}WCl_4(\mu\text{-dppm})_2$ is a unique example of a $W\overset{4}{-}WX_4(L\text{-}L)_2$ compound with a single $-CH_2-$ bridge and a torsional angle of 17.25°, quite similar to the angle observed in $Mo\overset{4}{-}MoCl_4(\mu\text{-dmdppm})_2$ [13]. However, as predicted for three atom ligand bridges, all of these complexes have relatively small torsional angles of less than 20° [3].

The strength of the $Mo\overset{4}{-}Mo$ bond is quite sensitive to the torsional angle [2] and is reflected in the length of the metal–metal bond. The δ^2 contribution to the quadruple bond varies as the cosine of 2χ with χ defined as the torsional angle with a maximum overlap at 0° and a minimum at 45°. For $Mo\overset{4}{-}MoCl_4(\mu\text{-dmdppm})_2$ with a torsional angle of 17.56°, the $Mo\overset{4}{-}Mo$ bond distance is 2.1523(9) Å, significantly longer than either $Mo\overset{4}{-}MoCl_4(\mu\text{-dppm})_2$ or $Mo\overset{4}{-}MoCl_4(\mu\text{-dmpm})_2$. The $Mo\overset{4}{-}Mo$ bond distances in $Mo\overset{4}{-}MoCl_4(\mu\text{-dppm})_2$ and $Mo\overset{4}{-}MoCl_4(\mu\text{-dmpm})_2$ are 2.138 and 2.125 Å, respectively. The $Mo\overset{4}{-}Mo$ distance in $Mo\overset{4}{-}MoCl_4(\mu\text{-dmpm})_2$ is slightly shorter than for $Mo\overset{4}{-}MoCl_4(\mu\text{-dppm})_2$ (0.013 Å). While this may be due to steric factors, it is also possible that the greater basicity of the phosphorus atoms in dmpm causes this shortening for electronic reasons. Since one would predict the bond distance of $Mo\overset{4}{-}MoCl_4(\mu\text{-dmdppm})_2$ to fall between the $Mo\overset{4}{-}Mo$ distance of $Mo\overset{4}{-}MoCl_4(\mu\text{-dppm})_2$ and $Mo\overset{4}{-}MoCl_4(\mu\text{-dmpm})_2$ based on the properties of the phosphine ligand, the lengthening of the $Mo\overset{4}{-}Mo$ bond is probably due to the presence of the twist along the $Mo\overset{4}{-}Mo$ axis.

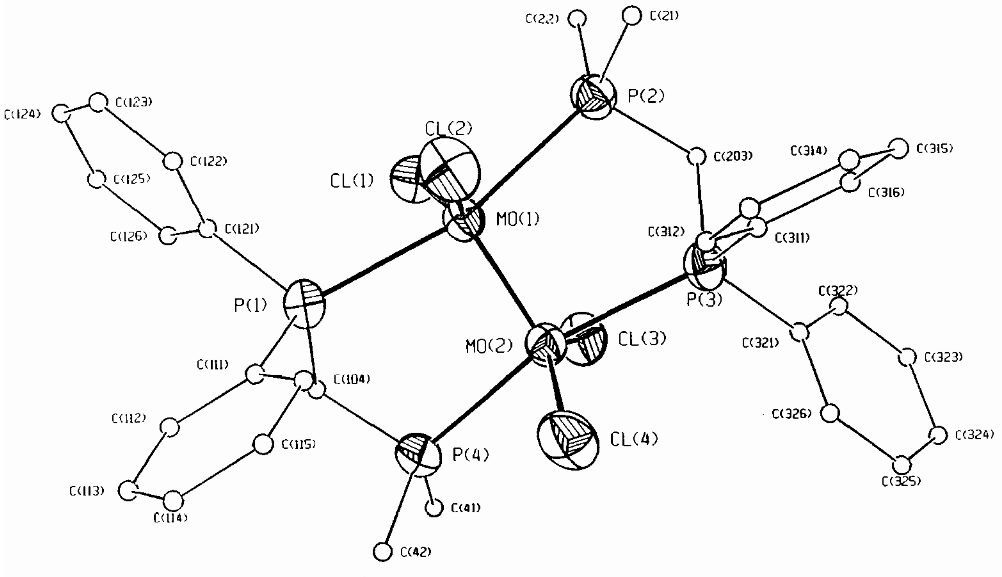

Fig. 1. An ORTEP drawing of $Mo\overset{4}{-}MoCl_4(\mu\text{-dmdppm})_2$. Thermal ellipsoids for Mo, Cl and P atoms are shown at 50% probability. The carbon atoms are shown as arbitrarily sized uniform circles.

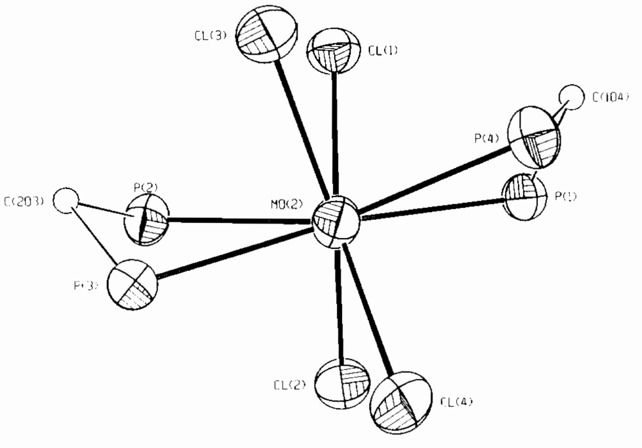

Fig. 2. An ORTEP drawing of the core atoms in $\mathrm{Mo}\overset{4}{-}\mathrm{MoCl_4}(\mu\text{-dmdppm})_2$ viewed down the $\mathrm{Mo}\overset{4}{-}\mathrm{Mo}$ axis showing the torsional angle. Thermal ellipsoids for Mo, Cl and P atoms are shown at 50% probability. The carbon atoms are shown as arbitrarily sized uniform circles.

TABLE 3. Summary of the individual torsional angles for $\mathrm{Mo}\overset{4}{-}\mathrm{MoCl_4}(\mu\text{-dmdppm})_2$ (°)

Cl(1)–Mo(1)–Mo(2)–Cl(3)	19.63 (0.08)
Cl(2)–Mo(1)–Mo(2)–Cl(4)	17.70 (0.10)
P(1)–Mo(1)–Mo(2)–P(4)	15.31 (0.07)
P(2)–Mo(1)–Mo(2)–P(3)	17.59 (0.07)

Numbers in parenthesis are e.s.d.s in the least significant digit.

TABLE 4. Selected bond distances (Å) and angles (°) for $\mathrm{Mo}\overset{4}{-}\mathrm{MoCl_4}(\mu\text{-dmdppm})_2$

Bond distances			
Mo(1)–Mo(2)	2.1523(9)	P(1)–C(121)	1.825(6)
Mo(1)–Cl(1)	2.400(2)	P(2)–C(21)	1.818(9)
Mo(1)–Cl(2)	2.390(2)	P(2)–C(22)	1.820(8)
Mo(1)–P(1)	2.558(2)	P(2)–C(203)	1.830(7)
Mo(1)–P(2)	2.582(2)	P(3)–C(203)	1.827(8)
Mo(2)–Cl(3)	2.401(2)	P(3)–C(311)	1.813(6)
Mo(2)–Cl(4)	2.394(2)	P(3)–C(321)	1.821(5)
Mo(2)–P(3)	2.544(2)	P(4)–C(41)	1.823(9)
Mo(2)–P(4)	2.570(2)	P(4)–C(42)	1.801(9)
P(1)–C(104)	1.820(8)	P(4)–C(104)	1.823(8)
P(1)–C(111)	1.814(6)		
Bond angles			
Mo(2)–Mo(1)–Cl(1)	106.06(5)	Cl(3)–Mo(2)–P(4)	85.60(7)
Mo(2)–Mo(1)–Cl(2)	112.20(7)	Cl(4)–Mo(2)–P(3)	90.37(8)
Mo(2)–Mo(1)–P(1)	96.46(5)	Cl(4)–Mo(2)–P(4)	89.11(8)
Mo(2)–Mo(1)–P(2)	98.47(5)	P(3)–Mo(2)–P(4)	163.42(7)
Cl(1)–Mo(1)–Cl(2)	141.72(8)	C(104)–P(1)–C(111)	103.2(3)
Cl(1)–Mo(1)–P(1)	82.02(7)	C(104)–P(1)–C(121)	106.7(3)
Cl(1)–Mo(1)–P(2)	86.07(7)	C(111)–P(1)–C(121)	102.7(2)
Cl(2)–Mo(1)–P(1)	92.38(7)	C(21)–P(2)–C(22)	101.5(4)
Cl(2)–Mo(1)–P(2)	89.48(8)	C(21)–P(2)–C(203)	106.1(4)
P(1)–Mo(1)–P(2)	163.00(7)	C(22)–P(2)–C(203)	102.4(4)
Mo(1)–Mo(2)–Cl(3)	104.93(6)	C(203)–P(3)–C(311)	104.0(3)
Mo(1)–Mo(2)–Cl(4)	112.41(7)	C(203)–P(3)–C(321)	107.1(3)
Mo(1)–Mo(2)–P(3)	96.35(6)	C(311)–P(3)–C(321)	101.9(2)
Mo(1)–Mo(2)–P(4)	99.16(6)	C(41)–P(4)–C(42)	102.3(5)
Cl(3)–Mo(2)–Cl(4)	142.65(8)	C(41)–P(4)–C(104)	103.3(4)
Cl(3)–Mo(2)–P(3)	84.79(7)	C(42)–P(4)–C(104)	105.3(4)

Numbers in parenthesis are e.s.d.s in the least significant digit.

While weakening the δ^2 bond, rotation about the $\mathrm{Mo}\overset{4}{-}\mathrm{Mo}$ axis also decreases repulsive forces between non-bonded atoms and the preferred conformation of a five- or six-membered ring may be established. A balance between the maximum $\mathrm{Mo}\overset{4}{-}\mathrm{Mo}$ orbital overlap and the minimum steric interaction is reflected in the torsional angle, but the twist may also be influenced by intermolecular packing forces [4]. However, it is not yet possible to predict whether a particular complex will have a torsional angle before any characterization of the complex has been done.

Table 4 lists selected bond distances and angles for $\mathrm{Mo}\overset{4}{-}\mathrm{MoCl_4}(\mu\text{-dmdppm})_2$. There is very little change in the metal to ligand bond distances with a change in the phosphine ligand from dppm to dmdppm to dmpm. For comparison, the average Mo–P distances for $\mathrm{Mo}\overset{4}{-}\mathrm{MoCl_4}(\mu\text{-dppm})_2$, $\mathrm{Mo}\overset{4}{-}\mathrm{MoCl_4}(\mu\text{-dmdppm})_2$ and $\mathrm{Mo}\overset{4}{-}\mathrm{MoCl_4}(\mu\text{-dmpm})_2$ are 2.58, 2.56 and 2.55 Å, and the Mo–Cl distances are 2.39, 2.40 and 2.41 Å, respectively [4, 5]. Unlike the $\mathrm{Mo}\overset{4}{-}\mathrm{Mo}$ bond distances, the metal–ligand distances for the dmdppm complex are intermediate to those of $\mathrm{Mo}\overset{4}{-}\mathrm{MoCl_4}(\mu\text{-dppm})_2$ and $\mathrm{Mo}\overset{4}{-}\mathrm{MoCl_4}(\mu\text{-dmpm})_2$. There are two crystalline forms of $\mathrm{Mo}\overset{4}{-}\mathrm{MoCl_4}(\mu\text{-dmpm})_2$, monoclinic and tetragonal. Due to the presence of disorder in the crystal structure of the tetragonal form, the bond distances of the monoclinic form have been used here for comparison [5].

UV–Vis spectroscopy

The 640 nm band in the UV–Vis spectrum of $\mathrm{Mo}\overset{4}{-}\mathrm{MoCl_4}(\mu\text{-dmdppm})_2$ is attributed to the $\delta^2 \rightarrow (\delta\delta^*)$ transition. The analogous bands occur at 634 and 604 nm in $\mathrm{Mo}\overset{4}{-}\mathrm{MoCl_4}(\mu\text{-dppm})_2$ and $\mathrm{Mo}\overset{4}{-}\mathrm{MoCl_4}(\mu\text{-dmpm})_2$ [4, 5]. The difference in the $\delta^2 \rightarrow (\delta\delta^*)$ transition in $\mathrm{Mo}\overset{4}{-}\mathrm{MoCl_4}(\mu\text{-dmpm})_2$ and $\mathrm{Mo}\overset{4}{-}\mathrm{MoCl_4}(\mu\text{-dppm})_2$ is attributed to the change in basicity of the bidentate phosphine ligands. However, the wavelength of the same transition of $\mathrm{Mo}\overset{4}{-}\mathrm{MoCl_4}(\mu\text{-dmdppm})_2$ does not fall between the transitions of $\mathrm{Mo}\overset{4}{-}\mathrm{MoCl_4}(\mu\text{-dppm})_2$ and $\mathrm{Mo}\overset{4}{-}\mathrm{MoCl_4}(\mu\text{-dmpm})_2$. The change in wavelength of the $\delta^2 \rightarrow (\delta\delta^*)$ transition is probably due to the presence of a torsional angle weakening the δ^2 bond. This is reflected in the lengthening of the $\mathrm{Mo}\overset{4}{-}\mathrm{Mo}$ bond and the red shift in wavelength of the $\delta^2 \rightarrow (\delta\delta^*)$ transition of the dmdppm complex relative to either $\mathrm{Mo}\overset{4}{-}\mathrm{MoCl_4}(\mu\text{-dppm})_2$ or $\mathrm{Mo}\overset{4}{-}\mathrm{MoCl_4}(\mu\text{-dmpm})_2$.

$^{31}P\{^1H\}$ *NMR analysis*

Since all the phosphorus atoms are equivalent in both $\mathrm{Mo}\overset{4}{-}\mathrm{MoCl_4}(\mu\text{-dppm})_2$ and $\mathrm{Mo}\overset{4}{-}\mathrm{MoCl_4}(\mu\text{-dmpm})_2$, the $^{31}\mathrm{P}\{^1\mathrm{H}\}$ NMR spectra are singlets at δ 16.04 and δ -0.77 ppm, respectively [5, 14]. Due to the presence of an asymmetric bidentate phosphine ligand with the head to tail arrangement shown in Fig. 1, the $^{31}\mathrm{P}\{^1\mathrm{H}\}$ NMR spectrum of $\mathrm{Mo}\overset{4}{-}\mathrm{MoCl_4}(\mu\text{-dmdppm})_2$ is more complex. The AA′BB′ pattern of the $^{31}\mathrm{P}\{^1\mathrm{H}\}$ NMR spectrum at room temperature consists of two complex multiplets with large J(P–P) couplings centered at δ 17.17 and δ -3.26 ppm. The coupling between the two phosphorus atoms in the free phosphine dmdppm is 104 Hz and the complex $\mathrm{Cl_2(PMe_2Ph)(PPH_3)Mo}\overset{4}{-}\mathrm{WCl_2(PMe_2Ph)_4}$, for example, has coupling between the two different *trans* phosphorus ligands on the molybdenum center of 141 Hz [15, 16]. Based on the chemical shifts of the free phosphines ($\mathrm{PPh_3} = \delta$ -5.4 ppm and $\mathrm{PMe_3} = \delta$ -62.2 ppm) [15] and the $^{31}\mathrm{P}\{^1\mathrm{H}\}$ NMR chemical shifts of $\mathrm{Mo}\overset{4}{-}\mathrm{MoCl_4}(\mu\text{-dppm})_2$ and $\mathrm{Mo}\overset{4}{-}\mathrm{MoCl_4}(\mu\text{-dmpm})_2$, the downfield shift may be assigned to the $-\mathrm{PPh_2}$ end and the upfield shift to the $-\mathrm{PMe_2}$ end of the ligand bound to the dimolybdenum core.

Supplementary material

Complete tables of crystal data, positional and isotropic equivalent thermal parameters, anisotropic thermal parameters, bond distances, bond angles and torsional angles for the molecule (10 pages); and listings of observed and calculated structure factors (19 pages) are available from author F.A.C. upon request.

Acknowledgement

We are grateful to the National Science Foundation for Support.

References

1 F. L. Campbell, F. A. Cotton and G. L. Powell, *Inorg. Chem., 24* (1985) 177.
2 F. A. Cotton and G. L. Powell, *Inorg. Chem., 22* (1983) 1507.
3 F. L. Campbell, F. A. Cotton and G. L. Powell, *Inorg. Chem., 23* (1984) 4222.
4 E. H. Abbott, K. S. Bose, F. A. Cotton, W. T. Hall and J. C. Sekutowski, *Inorg. Chem., 17* (1978) 3240.
5 F. A. Cotton, L. R. Falvello, W. S. Harwood, G. L. Powell and R. A. Walton, *Inorg. Chem., 25* (1986) 3949.
6 F. A. Cotton, M. W. Extine, T. R. Felthouse, B. W. S. Kolthammer and D. G. Lay, *J. Am. Chem. Soc., 103* (1981) 4040.
7 R. Uriarte, T. J. Mazanec, K. D. Tau and D. W. Meek, *Inorg. Chem., 19* (1980) 79.
8 A. Bino, F. A. Cotton and P. E. Fanwick, *Inorg. Chem., 18* (1979) 3558.
9 A. C. T. North, D. A. Phillips and F. S. Matthews, *Acta Crystallogr., Sect. A, 24* (1968) 351.
10 F. A. Cotton and S. Kitagawa, *Polyhedron, 7* (1988) 1673.
11 F. A. Cotton, L. R. Falvello, D. R. Root, T. J. Smith and K. Vidyasagar, *Inorg. Chem., 29* (1990) 1328.
12 J. D. Chen, F. A. Cotton and E. C. DeCanio, *Inorg. Chim. Acta, 176* (1990) 215.
13 J. M. Canich and F. A. Cotton, *Inorg. Chim. Acta, 142* (1988) 69.
14 F. A. Cotton, J. L. Eglin and C. A. James, *Inorg. Chem.,* (1992) submitted for publication.
15 H. Karsch and H. Schmidbaur, *Z. Naturforsch., Teil B, 32* (1977) 762.
16 F. A. Cotton, L. R. Favello, R. L. Luck, and C. A. James, *Inorg. Chem., 29* (1990) 4759.